

New Adjustable Slot Meander Patch Antenna for 4G Handheld Devices

Nassrin Ibrahim Mohamed Elamin, Tharek Abd Rahman, and Amuda Yusuf Abdulrahman

Abstract—Two different antennas constructed using a new concept, the slot meander patch (SMP) design, are presented in this study. SMP antennas are designed for fourth-generation long-term evolution (4G LTE) handheld devices. These antennas are used for different target specifications: LTE-Time Division Duplex and LTE-Frequency Division Duplex (LTE TDD and LTE FDD). The first antenna is designed to operate in a wideband of 1.68–3.88 GHz to cover eight LTE TDD application frequency bands. Investigations have shown that the antenna designed with unequal meander widths has a higher efficiency compared to its equivalent antenna design with equal meander widths. The second antenna was configured as a multiband SMP antenna, which operates at three distinct frequency bands (0.5–0.75, 1.1–2.7, and 3.3–3.9 GHz), to cover eight LTE FDD application bands including the lowest and the highest bands. There is a good agreement between the measurement and simulation results for both antennas. Moreover, parametric studies have been carried out to investigate the flexible multiband antenna. Results have shown that the bandwidths can be improved through adjusting the meander widths without changing the SMP length and all other parameters.

Index Terms—LTE antenna, LTE-FDD frequency bands, LTE-TDD frequency bands, slot meander patch.

I. INTRODUCTION

THE SOLUTION to the next-generation user equipment antennas is either a wideband or multiband antenna design [1]. Two possible designs are presented in this letter using the slot meander patch (SMP) antenna design. The first design operates as a wideband antenna, covering eight Long Term Evolution time division duplex (LTE TDD) application frequency bands; while the second one is an SMP multiband antenna, operating at three separate frequency bands. The adjustable SMP antenna, as shown in Fig. 1(a), can be set by adjusting such parameters as slot width, radiator width, meander magnitude (antenna length), and antenna meander widths.

II. WIDEBAND SMP ANTENNA

The conventional meander-line antennas are typically distinguished by a wide bandwidth (BW), compared to other small monopole antenna alternatives [2], [3]. For instance in [4], a BW of 910 MHz has been achieved in a LTE mobile phone antenna with a size of $200 \times 44 \text{ mm}^2$. The BW can further be improved by constructing narrow parallel slots over a meander patch. The

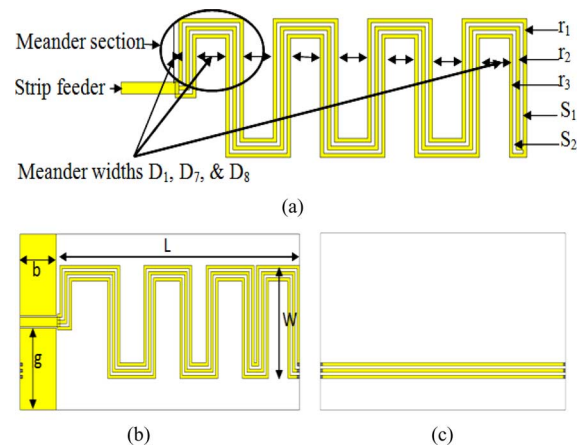


Fig. 1. (a) Geometry of the slot meander radiator. (b) Front view and CPW dimensions. (c) Back view of the simulated wideband antenna.

matching impedance BW can be improved by the generated parallel meander lines and capacities in between. A wideband SMP antenna is introduced in this letter for improving the conventional meander-line antennas' BW to 2.2 GHz, with a size of $100 \times 35 \text{ mm}^2$ and BW ratio of 79%.

A. Wideband SMP Antenna Design

The proposed wideband antenna (Fig. 1) is designed on two surfaces of a low-cost FR-4 substrate (relative permittivity $\epsilon_r = 4.7$, loss tangent $\delta = 0.02$, and thickness of 1.6 mm). The antenna's size ($L \times W \times H$) is $100 \times 35 \times 1.635 \text{ mm}^3$. The main radiator is a simple printed planar meander patch slotted with two parallel continuous meander slots, S_1 and S_2 , with a width of 1 mm. The slots serve to distribute the meander patch to three parallel meander lines connected at the edges. Three lines extend over the antenna's back side with zero meander magnitude. This is aimed at shortening the main radiator to the coplanar waveguide (CPW) design's ground plane. The meander wire antenna invented in [5] was tested by varying such design variables as the number of sections per wavelength N and antenna reduction ratio β . Note that $\beta = \mu/\lambda$, where μ and λ are the reduced length after meander and overall wire length, respectively. It was found that the antenna performances were improved by decreasing the value of N . However, resonant resistance and BW decrease as β decreases. Therefore, in most of the recently published research works, two-section designs were proposed for print planar meander-line antenna designs [4], [6]. Consequently, the proposed design has two sections per wavelength ($N = 2$) as shown in Fig. 1(a). The section length (m) is 18 mm, which is equivalent to 0.1λ of 1.68 GHz (the lowest frequency). The optimized design parameters of the proposed

Manuscript received June 28, 2013; accepted August 25, 2013. Date of publication September 04, 2013; date of current version September 13, 2013.

The authors are with the Wireless Communication Centre (WCC), Electrical Engineering (FKE), Universiti Teknologi Malaysia, 81300 Johor Bahru, Malaysia (e-mail: nisreenalameen@gmail.com).

Color versions of one or more of the figures in this letter are available online at <http://ieeexplore.ieee.org>.

Digital Object Identifier 10.1109/LAWP.2013.2280029

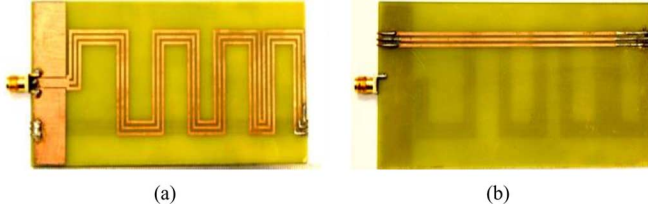


Fig. 2. Optimized model of the fabricated antenna: (a) face view and (b) back view.

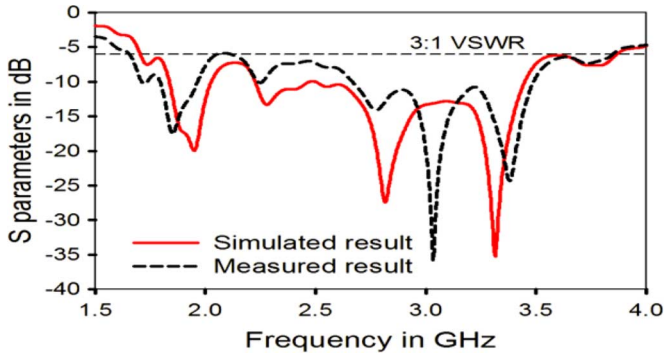


Fig. 3. Simulated and measured S -parameters for the wideband SMP antenna.

TABLE I
DESIGN PARAMETERS FOR THE WIDEBAND SMP ANTENNA ELEMENTS
(UNITS: MILLIMETERS)

$R_1=1$	$W=35$	$D_4=6$
$R_2=1$	$T=1.6$	$D_5=10$
$R_3=1$	$H=1.635$	$D_6=10$
$S_1=1$	$D_1=8$	$D_7=15$
$S_2=1$	$D_2=1$	$D_8=1$
$L=100$	$D_3=10$	$M=18$

SMP wideband antenna' elements are shown in Fig. 1(b) and (c) and detailed in Table I.

B. Experimental Results of Wideband SMP Antenna

The proposed SMP wideband antenna was simulated using CST Microwave Studio software, while the Agilent Technologies vector network analyzer E5071C was used for measuring the fabricated antenna's return loss. There is good agreement between the simulation and measurement results. The fabricated antenna prototype is shown in Fig. 2, while both measured and simulated return losses are shown in Fig. 3. Note that the BW definition of 3:1 VSWR (-6 dB return loss) is widely used as the design specifications of hand user equipment antennas [7], [8]. As shown in Table II, the proposed design can match the eight LTE TDD application frequency bands. Fig. 4 has also shown that it is possible to achieve efficiency greater than 50%. The antenna efficiency was computed as follows:

$$\text{Efficiency} = \frac{G(\theta, \phi)}{D(\theta, \phi)}(1 - |\Gamma|^2) \quad (1)$$

where G and Γ are the measured gain in decibels and reflection coefficient, respectively; while the directivity (D) was computed using the radiation intensity. There is good agreement

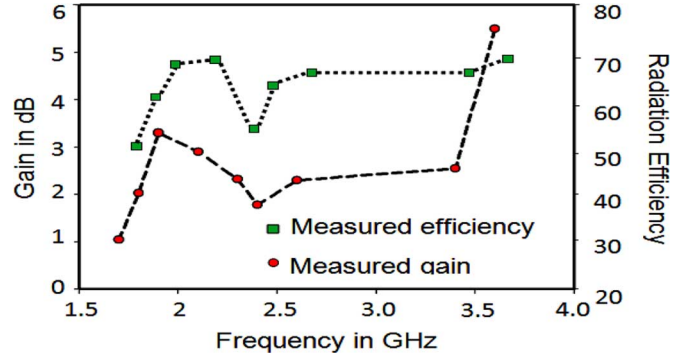


Fig. 4. Measured efficiency and gain of the SMP wideband antenna.

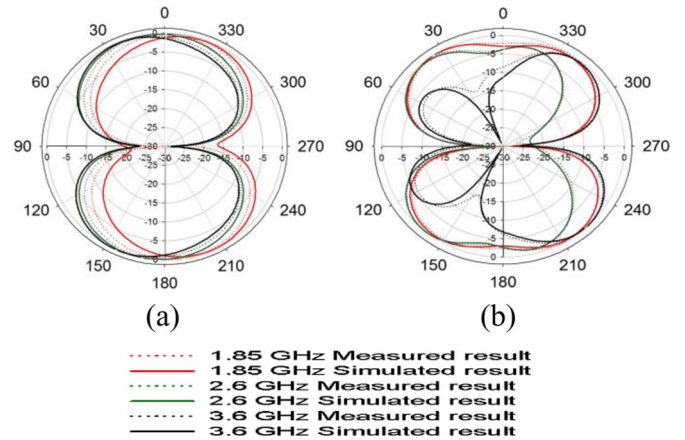
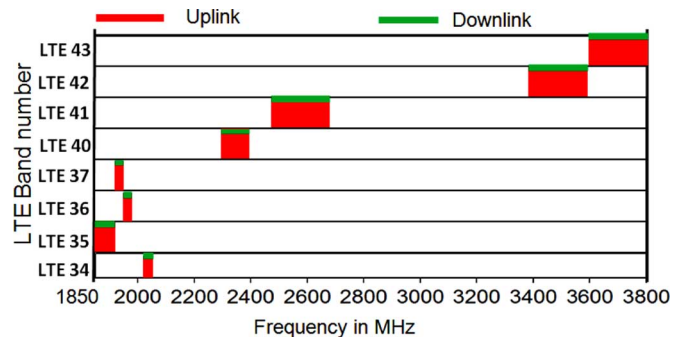


Fig. 5. Proposed SMP wideband antenna's measured and simulated (a) E-planes and (b) H-planes.

TABLE II
WIDEBAND SMP ANTENNA SPECTRUM



between measured and simulated E- and H-planes for the proposed antenna, as shown in Fig. 5.

C. Comparison Between Equal and Unequal Meander Widths

The proposed wideband SMP antenna has unequal meander widths, contrary to the conventional meander-line antennas which are typically designed to have equal meander widths [2], [4], [6]. The two different designs (equal and unequal meander widths) are compared in this section. The two have similar lengths ($\sum_{i=1}^n D_n = 61$ mm where $n = i = 1, 2, 3 \dots 8$), with all other parameters being identical, with the exception of meander widths. This study has revealed that the two designs (herein compared) have slightly different

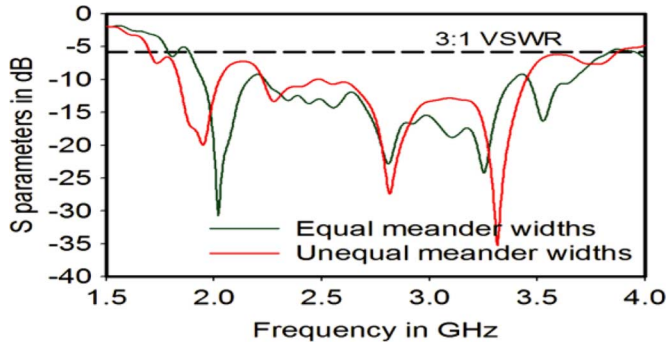
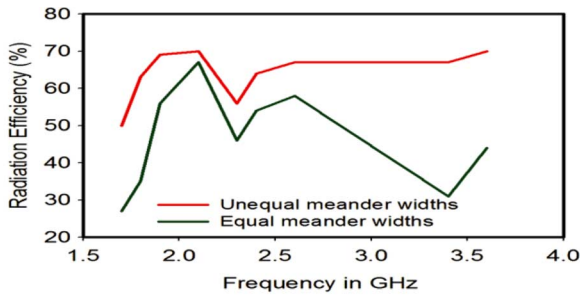
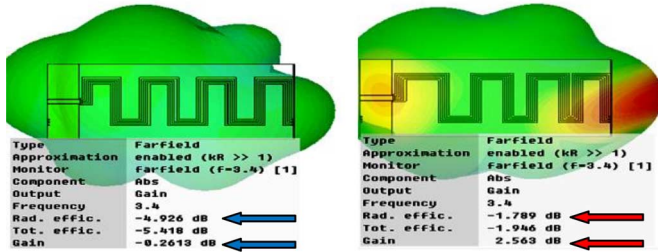


Fig. 6. Comparison between simulated S -parameters of equal and unequal meander designs.



(a)



(b)

(c)

Fig. 7. (a) Comparison between simulated efficiencies of the equal and unequal meander designs. (b), (c) Simulated 3.4-GHz radiation pattern showing the efficiencies in equal and unequal meander respectively (31% and 67%).

matched frequency BWs, as shown in Fig. 6. The antenna's efficiency is reduced in equal meander design, compared to its counterpart unequal meander design, as shown in Fig. 7(a) and (b). This is due to adjustment of meander widths, in which the antenna's radiation characteristics are affected by the amount of generated electrical capacities within distances D_n (where $n = 1, 2, \dots, 8$).

III. MULTIBAND SMP ANTENNA

Multiband antennas can be constructed by creating slots over patch antennas [3]. Therefore, an SMP multiband antenna (Fig. 8) is introduced in order to show the electrical and mechanical flexibilities of the proposed SMP design. This is possible, as the matched impedance BW can be altered by the amount of generated capacity within distances D_n , by adjusting meander widths and magnitude. The second slot meander antenna is adjusted as a multiband antenna that operates at three distinct frequency bands (0.5–0.75, 1.1–2.7, and 3.3–3.9 GHz), thus covering the eight LTE FDD bands, as shown in Table III and Fig. 9.

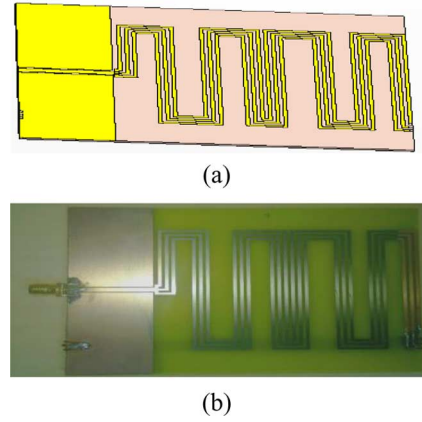


Fig. 8. (a) Simulated antenna and (b) prototype of fabricated SMP multiband antenna.

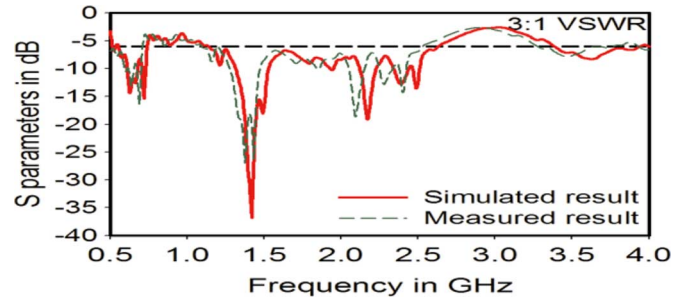
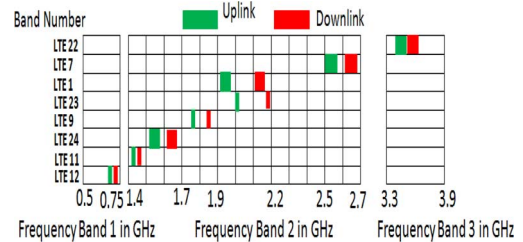


Fig. 9. Simulated and measured S -parameters of proposed wideband SMP antenna (NB: the antenna matches three distinct bands).

TABLE III
MULTIBAND SMP ANTENNA COVERED BANDS CONCEPT



A. Multiband SMP Antenna Design

The SMP multiband antenna can match three distinct frequency bands by adjusting the slot antenna's meander widths (D_1, D_2, \dots, D_8) to $D_1 = 5$ mm, $D_2 = 5$ mm, $D_3 = 8$ mm, $D_4 = 1$ mm, $D_5 = 6$ mm, $D_6 = 7$ mm, $D_7 = 5$ mm, and $D_8 = 1$ mm. Next, the meander magnitude is adjusted to 15 mm, which is 0.025λ of the multiband antenna lower frequency (0.5 GHz), while the SMP multiband antenna dimensions are 80×60 mm².

B. Experimental Results and Discussions

The SMP multiband antenna was also simulated using CST Microwave Studio software. When compared, there is good agreement between the simulated and measured return losses, as shown in Fig. 9. Three distinct frequency bands (0.5–0.75, 1.1–2.7, and 3.3–3.9 GHz) were obtained, as also shown in Fig. 9. The antenna's measured efficiency and gain are shown

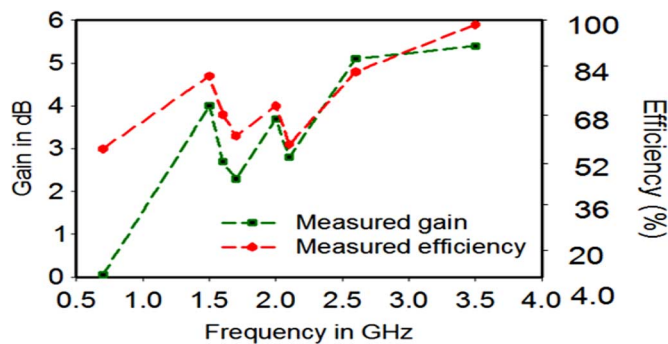


Fig. 10. SMP multiband antenna's measured efficiency and gain.

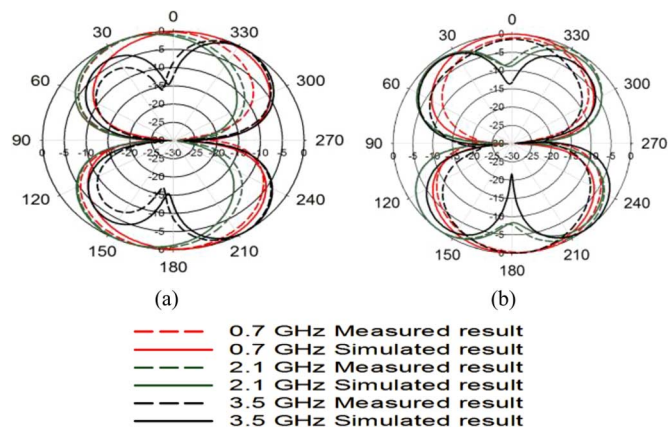


Fig. 11. SMP antenna's measured and simulated three distinct bands. (a) E-planes and (b) H-planes.

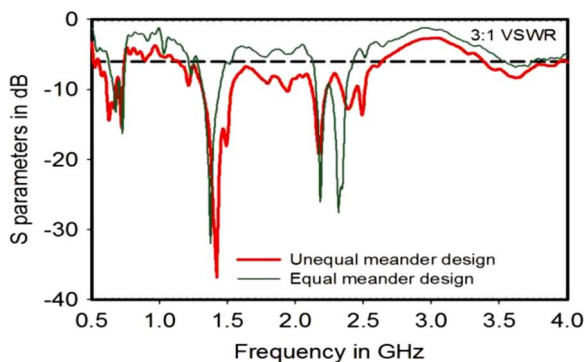


Fig. 12. Simulated S -parameters for improving the covered BWs.

in Fig. 10, while the simulated and measured radiation pattern characteristics are shown in Fig. 11.

C. Meander Widths Adjustment for BW Improvement

The SMP multiband antenna design also has unequal meander widths. The equal meander width and unequal meander width multiband designs are compared in this section. The two designs have similar lengths, with all other parameters also being identical, except the meander widths. It has been shown in this study that the matched frequency BWs can be improved only by adjusting the meander widths, while keeping

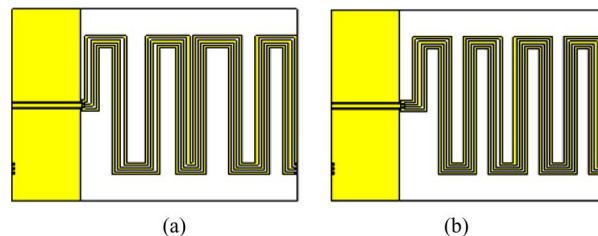


Fig. 13. Geometry of the multiband SMP antenna (a) simulated unequal meander design and (b) equal meander design.

SMP length and all other parameters unaltered. This showed the electrical and mechanical flexibilities of the proposed SMP design. The simulated return losses for equal meander and its counterpart unequal meander designs are shown in Fig. 12, while the geometry of multiband SMP antenna are shown in Fig. 13(a) and (b) for simulated unequal meander design and equal meander design, respectively.

IV. CONCLUSION

The proposed multiband SMP antennas have been simulated, fabricated, and tested; there is good agreement between the measurement and simulation results. The slot designs over the meander patch show wide BW of greater than 2 GHz. The SMP antenna designed with unequal meander widths shows an increase in radiation efficiency compared to its counterpart design using equal meander widths. Therefore, the proposed SMP multiband antenna seems to offer significant improvements (higher BW and increased radiation efficiency), compared to the conventional meander-line antennas. Moreover, the SMP antenna is both electrically and mechanically flexible, and therefore its matched frequency BWs of the SMP multiband antenna can be improved only by adjusting the meander widths, without altering either SMP length or any other parameters.

REFERENCES

- [1] M. Secmen, "Multiband and wideband antennas for mobile communication systems," in *Recent Developments in Mobile Communications—A Multidisciplinary Approach*. New York, NY, USA: InTech, 2011, pp. 143–163.
- [2] O. O. Olaode, W. D. Palmer, and W. T. Joines, "Characterization of meander dipole antennas with a geometry-based, frequency-independent lumped element model," *IEEE Antennas Wireless Propag. Lett.*, vol. 11, pp. 346–349, 2012.
- [3] D. A. Sánchez-Hernández, *Multiband Integrated Antennas for 4G Terminals*. Norwood, MA, USA: Artech House, 2008.
- [4] S. L. Zuo, Z. Y. Zhang, and J. W. Yang, "Planar meander monopole antenna with parasitic strips and sleeve feed for DVB-H/LTE/GSM850/900 operation in the mobile phone," *IEEE Antennas Wireless Propag. Lett.*, vol. 12, pp. 27–30, 2013.
- [5] J. Rashed and C. T. Tai, "A new class of resonant antennas," *IEEE Trans. Antennas Propag.*, vol. 39, no. 9, pp. 1428–1430, Sep. 1991.
- [6] S. Ghosh, T. N. Tran, and T. Le-Ngoc, "Miniaturized four-element diversity PIFA," *IEEE Antennas Wireless Propag. Lett.*, vol. 12, pp. 396–400, 2013.
- [7] K. Byeongkwan *et al.*, "Isolation enhancement of USB dongle MIMO antenna in LTE 700 band applications," *IEEE Antennas Wireless Propag. Lett.*, vol. 11, pp. 961–964, 2012.
- [8] B. Yong-Ling, C. Jin-Hua, S. Si-Cheng, J. L. W. Li, and G. Jin-Hong, "Printed monopole antenna with a long parasitic strip for wireless USB dongle LTE/GSM/UMTS operation," *IEEE Antennas Wireless Propag. Lett.*, vol. 11, pp. 767–770, 2012.